Materials Science Research International, Vol.5, No.3 pp.189-194 (1999)

General paper

A MICROMECHANICAL MODELING APPROACH TO THE MECHANICAL PROPERTIES OF TEXTILE ELASTOMERIC COMPOSITES

Zheng Ming HUANG, Seeram RAMAKRISHNA and Andrew A.O. TAY

Department of Mechanical & Production Engineering
National University of Singapore, 10 Kent Ridge Crescent, Singapore 119260

Abstract: Elastomer-based fibrous composites are characterized by a significantly nonlinear whilst usable deformation range under external loads, which provides a great challenge to the development of a constitutive description for the composites. This paper presents a micromechanical modeling approach to the entire stress-strain response of such composites based on knowledge of constituent fiber and matrix properties only. A new and accurate rubber-elasticity theory is applied to describe stress-strain behavior of the elastomer matrix material. A bridging model is used to determine internal stresses generated in the constituent materials, and the overall compliance matrix of the composite at each load level follows easily. The proposed model has been applied to an interlock weft knitted polyester fiber fabric reinforced polyurethane matrix composite. Reasonably good correlation has been found between the theoretical and experimental results.

Key words: *Mechanical properties, Micromechanical approach, Bridging model, Stress-strain response, Knitted fabric composites, Rubber-elasticity*

1. INTRODUCTION

Composites made from elastomers and textile fabrics are finding useful applications in many aspects of engineering. To use these materials efficiently, it is important to understand their mechanical properties. However, due to extreme complexity, there exist very limited number of micromechanical models for the non-linear stress-strain response characteristics of the textile elastomeric composites. Chou et al.[1,2] proposed a sinusoidal model to locate the fiber configuration in flexible composites under deformation. Although the geometrical nonlinearity has been considered, they used a classical lamina theory to derive the overall stiffness matrix of the composite, whereas the matrix's modulus was defined with the simple James and Guth's formula [3]. Hence, their approach is applicable only in a mode-rately small deformation range. To the best of our knowledge, a complete 3D (three-dimensional) micromechanical approach, based on understanding of the constituent material properties, to predict the entire nonlinear constitutive relationship of an elastomer-based textile composite has not been seen in the literature until to date.

This paper presents such a micromechanical modeling approach to characterise the stress-strain response of a textile elastomeric composite. A representative volume element (RVE) of the textile composite is divided into a number of sub-elements, each of which contains only one fiber segment. Such a sub-element is considered as a unidirectional composite, for which a bridging model is used to determine internal stresses generated in the constituent fiber and matrix materials. These stresses are explicitly expressed as functions of overall applied loads, and hence constitutive equations of the composite at every load level follows directly. A new and accurate rubber elasticity theory is applied to describe the constitutive equations of the elastomer matrix. The overall property of the textile composite is then obtained by assembling contributions of all the sub-elements. Predicted results of an interlock polyester fiber fabric reinforced polyurethane elastomer composite agree favourably with experiments.

2. THEORY

Consider a unidirectional fiber reinforced elastomer matrix composite. The best way to tailor any large deformation is to express the stress-strain relationship in an incremental form. Thus, the incremental constitutive equations of the fiber, matrix, and the composite are expressed as

$$\{d\varepsilon_i^{f}\}=[S_{ij}^{f}]\{d\sigma_j^{f}\}, \quad (1)$$

$$\{d\varepsilon_i^{m}\}=[S_{ij}^{m}]\{d\sigma_j^{m}\}, \quad (2)$$

$$\{d\varepsilon_i\}=[S_{ij}]\{d\sigma_j\}, \quad (3)$$

where and in the following m and f refer to the matrix and the fiber, respectively, with a quantity without any suffix denoting the composite. $\{d\sigma_i\}=\{d\sigma_{11}, d\sigma_{22}, d\sigma_{33}, d\sigma_{23}, d\sigma_{13}, d\sigma_{12}\}^T$, $\{d\varepsilon_i\}=\{d\varepsilon_{11}, d\varepsilon_{22}, d\varepsilon_{33}, 2d\varepsilon_{23}, 2d\varepsilon_{13}, 2d\varepsilon_{12}\}^T$, and $[S_{ij}^f]$, $[S_{ij}^m]$, and $[S_{ij}]$ are the compliance matrices of the fiber, matrix, and the composite materials, respectively. The volume averaged stress and strain increments satisfy

$$\{d\sigma_i\}=V_f\{d\sigma_i^{f}\}+V_m\{d\sigma_i^{m}\}, \quad (4)$$

Received November 25, 1998
Accepted August 10, 1999

$$\{d\varepsilon_i\}=V_f\{d\varepsilon_i^f\}+V_m\{d\varepsilon_i^m\}, \quad (5)$$

where V_f and V_m are the volume fractions of the fiber and the matrix in the composite.

Suppose that the stress vectors of the fiber and the matrix are correlated by a bridging matrix through

$$\{d\sigma_i^m\}=[A_{ij}]\{d\sigma_j^f\}. \quad (6)$$

From Eqs. (1)-(6), we can easily obtain:

$$\{d\sigma_i^f\}=(V_f[I]+V_m[A_{ij}])^{-1}\{d\sigma_j\}, \quad (7)$$

$$\{d\sigma_i^m\}=[A_{ij}](V_f[I]+V_m[A_{ij}])^{-1}\{d\sigma_j\}, \quad (8)$$

$$[S_{ij}]=(V_f[S_{ij}^f]+V_m[S_{ij}^m][A_{ij}])(V_f[I]+V_m[A_{ij}])^{-1}. \quad (9)$$

The bridging matrix, $[A_{ij}]_{6\times6}$, depends on $[S_{ij}^f]$ and $[S_{ij}^m]$. When $[S_{ij}^f]$ and $[S_{ij}^m]$ are both described by Hooke's law, the non-zero elements (the others are all zero) of $[A_{ij}]_{6\times6}$ are given by[4-6]:

$$a_{11}=E_m/E_f, \quad (10)$$

$$a_{22}=a_{33}=0.5(1+E_m/E_f), \quad (11)$$

$$a_{55}=a_{66}=0.5(1+G_m/G_f), \quad (12)$$

$$a_{13}=a_{12}=(S_{12}^f-S_{12}^m)(a_{11}-a_{22})/(S_{11}^f-S_{11}^m), \quad (13)$$

$$a_{44}=\frac{V_f(G_{23}-G_f)G_m}{V_m(G_m-G_{23})G_f}, \quad (14)$$

where $G_{23}=\dfrac{(V_f+V_m a_{11})(V_f+V_m a_{22})^2}{2(d_1+d_2)}$, with

$$d_1=S_{22}^f[V_f^3+V_mV_f^2(a_{11}+a_{22})+V_fV_m^2a_{11}a_{22}]+S_{22}^m[V_fV_m(V_f+V_ma_{33}+V_ma_{11})a_{22}+V_m^3a_{11}a_{22}a_{33}]-V_fV_m(V_f+V_ma_{33})(S_{12}^f-S_{12}^m)a_{12},$$

$$d_2=V_fV_m(V_f+V_ma_{33})(S_{12}^f-S_{12}^m)a_{12}-S_{12}^f[V_f^3+V_fV_m(V_f+V_ma_{11})a_{22}]-S_{23}^m[V_fV_m(V_f+V_ma_{22}+V_ma_{11})a_{22}+V_m(V_f^2+V_m^2a_{22}a_{33})a_{11}].$$

Suppose that the fibers only exhibit elastic deformation, which is true for most knitted fabric reinforced elastomer composites. However, linear elasticity assumption is only valid in a very small deformation range for the elastomer matrix materials. To tailor large deformation of the elastomers, a hyper-elastic theory has to be incorporated. However, currently used hyper-elastic theories for elastomer or rubber-like solids are less satisfactory for the present application in two aspects[7]. Firstly, they use total stress-total strain description and the resulting constitutive equations are significantly non-linear especially when the global coordinates do not coincide with the principal stretch directions of the materials. Secondly, fitting the physical constants involved in these theories to uniaxial tension data, which are the most convenient to obtain, results in inaccurate or even unstable response in the other deformation modes [7]. As such, a new rubber-elasticity theory has been developed instead, and is applied to the present matrix material. This theory claims that the stress-strain relationship of the material at each load level is expressed by Eq. (2), where the compliance matrix, $[S_{ij}^m]$, is the same as that given by the Hooke's law but with varied Young's modulus and Poisson's ratio. The variations of the Young's modulus and Poisson's ratio are expressed as functions of a current effective strain that is defined using total strains as

$$\varepsilon_e=\sqrt{\frac{2}{3}\varepsilon_{ij}\varepsilon_{ij}}=\sqrt{\frac{2}{3}\left[\varepsilon_{11}^2+\varepsilon_{22}^2+\varepsilon_{33}^2+2\left(\varepsilon_{23}^2+\varepsilon_{13}^2+\varepsilon_{12}^2\right)\right]}$$
$$=\sqrt{\frac{2}{3}\left[\varepsilon_1^2+\varepsilon_2^2+\varepsilon_3^2+\frac{1}{2}\left(\varepsilon_4^2+\varepsilon_5^2+\varepsilon_6^2\right)\right]}. \quad (15)$$

Under uniaxial tension, $\varepsilon_1=\varepsilon_2$ and $J=(1+\varepsilon_1)(1+\varepsilon_2)\bullet(1+\varepsilon_3)\equiv1$ (incompressibility). Therefore, the Young's modulus, Poisson's ratio, and the effective strain are obtained as:

$$E^n=\frac{\sigma_u^n-\sigma_u^{n-1}}{\varepsilon_u^n-\varepsilon_u^{n-1}}, \quad (16)$$

$$\nu^n=\left[\frac{1}{\sqrt{1+\varepsilon_u^{n-1}}}-\frac{1}{\sqrt{1+\varepsilon_u^n}}\right]\Big/\left(\varepsilon_u^n-\varepsilon_u^{n-1}\right), \quad (17)$$

$$\varepsilon_e^n=\sqrt{\frac{2}{3}\left[\left(\varepsilon_u^n\right)^2+2\left(\frac{1}{\sqrt{1+\varepsilon_u^n}}-1\right)^2\right]}, \quad (18)$$

$n=1, 2, \dots$

where σ_u and ε_u $(=\varepsilon_1)$ are nominal tensile stress and strain, respectively, and the superscript n-1 refers to the previous load level. Thus, Eqs. (16) and (17) define two functions of E and ν upon ε_e at an arbitrary load level. As long as the effective strain in the material is determined from Eq. (18), the instantaneous Young's modulus and Poisson's ratio are obtainable and the constitutive equations of the material for the next load step calculation are described by Eq. (2).

The accuracy of this new rubber-elasticity theory and its superiority over other widely used hyper-elastic theories have been verified using Treloar's test data[8]. Predictions for biaxial and shear loads are shown in Figs. 1 and 2, respectively. In the figures, "incremental theory" refers to the present theory, whereas "polynomial model" denotes another widely used hyper-elastic theory for rubber-like solids[7]. It should be noted that the material parameters in both the models were fitted to uniaxial tension data only. Then, the models were applied to simulate the material response under equibiaxial tension (Fig. 1) and the response under pure shear (Fig. 2). More details about the incremental theory have been reported elsewhere[9].

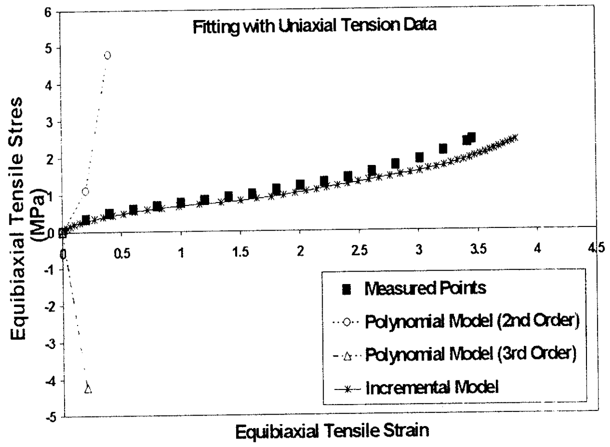

Fig. 1. Equibiaxial tension results of 8% sulfur rubber.

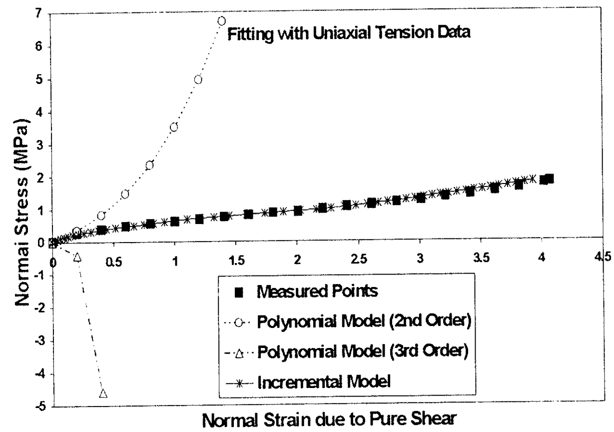

Fig. 2. Pure shear results of 8% sulfur rubber.

3. STRENGTH CRITERION

In predicting the stress-strain curve of the composite due to external loads, a strength criterion should be incorporated. This criterion will enable one to determine the extent of the predicted curve and the composite ultimate strength. As the stress-state in each constituent phase is explicitly known, and as strength theories for single-phase isotropic materials are well developed, setting a failure criterion is straightforward for the composite.

Based on Eqs. (7) and (8), the total stresses in the constituent fiber and the matrix are updated through

$$\{\sigma_i^{\mathrm{f}}\}=\{\sigma_i^{\mathrm{f}}\}+\{\mathrm{d}\sigma_i^{\mathrm{f}}\}, \quad (19)$$

$$\{\sigma_i^{\mathrm{m}}\}=\{\sigma_i^{\mathrm{m}}\}+\{\mathrm{d}\sigma_i^{\mathrm{m}}\}. \quad (20)$$

It is evident that the composite strength depends on the strengths of the constituent materials. Let us accept an assumption that when any constituent material attains its ultimate stress state, the corresponding applied overall stress is defined as the ultimate strength of the composite. This assumption will make the treatment of the composite strength quite easy.

All the strength theories for isotropic materials are developed based on three principal stresses. For a general stress state (σ_{xx}, σ_{yy}, σ_{zz}, σ_{yz}, σ_{xz}, σ_{xy}), the three principal stresses σ^1, σ^2, and σ^3, with $\sigma^1 \geq \sigma^2 \geq \sigma^3$, are the solutions to the following eigen-value equation.

$$\det\left(\begin{bmatrix}\sigma_{xx} & \sigma_{xy} & \sigma_{xz}\\ \sigma_{yx} & \sigma_{yy} & \sigma_{yz}\\ \sigma_{zx} & \sigma_{zy} & \sigma_{zz}\end{bmatrix} - \sigma[I]\right)=0.$$

One of the most successful strength theories of an isotropic material is the maximum normal stress theory, which says that the material fails as long as σ^1 reaches its ultimate value, no matter whether the material is under uniaxial or multiaxial state of stress. The failure criterion can be expressed as

$$\sigma^1 \geq \sigma_{\mathrm{u}} \quad (21)$$

where σ_{u} is the ultimate tensile strength of the material obtained from a uniaxial test. Based on Eq. (21), the composite strength can be determined accordingly.

4. EXPERIMENTAL DETAILS

Experiment has been carried out to fabricate a composite by reinforcing an interlock weft knitted polyester fiber fabric in a polyurethane matrix. The fabrication was conducted using a compression molding machine by hand lay-up method. After the compression, the fabric geometry became nearly two-dimensional. The coordinates of the yarns in a RVE (Fig. 3) of the composite were determined through measurement on microscope pictures of the composite pieces and the fiber volume fraction was obtained through a geometric technique[10]. Tensile tests were performed for the composite samples along the wale and the course directions, respectively. In this paper, the wale direction was taken as the global x-direction and the course as the global y-direction, see Fig. 3. The test results are summarized in Table 1 and are plotted in Figs. 4 and 5, respectively. In the table, E_{L} is the (linear) Young's modulus, σ_{L} and ε_{L} are the knee stress and knee strain (the limit points to which a linear elastic stress-strain relationship holds), and σ_{u} and ε_{u} are the ultimate stress and ultimate strain of the composite, respectively.

Table 1. Mechanical properties of the textile elastomeric composite

	Load in wale direction (V_f=0.362)		Load in course direction (V_f=0.354)	
	Measured	Predicted	Measured	Predicted
E_L(MPa)	192.43	241.2	71.4	70.6
σ_L(MPa)	4.05	4.65	1.77	1.15
σ_u(MPa)	50.52	51.67	20.86	9.72
ε_L (%)	2.1	1.93	2.49	1.63
ε_u(%)	86.23	93.19	127.48	77.72

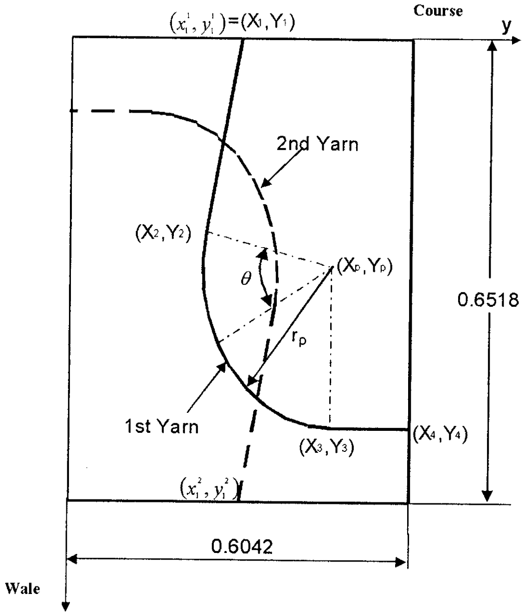

Fig. 3. RVE of the textile elastomeric composite. (a planar geometry with two yarns symmetric to each other, and with X_1=0.0, X_2=0.27, X_3=0.5414, X_4=0.5414, X_p=0.3141, Y_1=0.3021, Y_2=0.2416, Y_3=0.4635, Y_4=0.6042, and Y_p=0.4635)

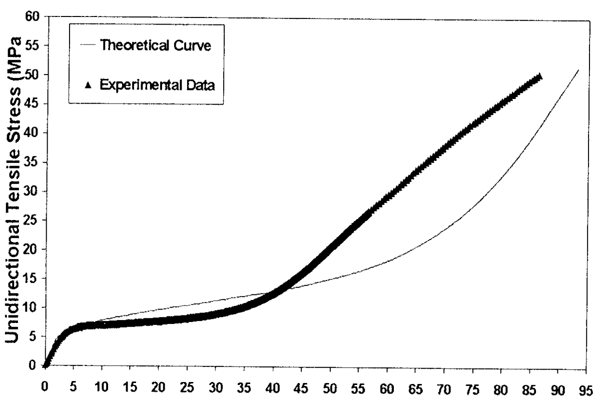

Fig. 4. Predicted and measured stress-strain curves in wale direction (V_f=0.362).

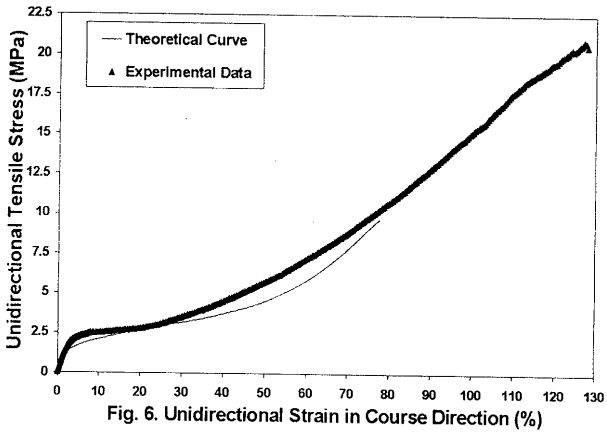

Fig. 5. Predicted and measured stress-strain curves in course direction (V_f=0.354).

Uniaxial tension tests were also carried out for the fiber and matrix materials to determine the constituent properties. Measured parameters for the polyester fibers are:E_f=6.04GPa and ν_f=0.42. Young's modulus, E_m, and Poisson's ratio, ν_m, of the polyurethane versus its effective strain were approximated using polynomials. Polynomial functions of order up to 17 were investigated. It was found that the 17th order polynomial gave a sufficiently good fit to the experimental data. The two 17th order polynomials to represent E_m and ν_m are given, respectively, by:

$$E_m(\varepsilon_e)=A_1+A_2(\varepsilon_e-\varepsilon_o)+A_3(\varepsilon_e-\varepsilon_o)^2+\cdots+A_{18}(\varepsilon_e-\varepsilon_o)^{17},$$

$$\varepsilon_e \leq \varepsilon_{eu}$$

A_1=+0.265953E+00, A_2=+0.664798E-01, A_3=-0.379756E-01, A_4=+0.466002E-01, A_5=+0.948304E-01, A_6=-0.312507E-01, A_7=-0.463988E-01, A_8=+0.113865E-01, A_9=+0.110157E-01, A_{10}=-0.231237E-02, A_{11}= -0.140701E-02, A_{12}=+0.270237E-03, A_{13}=+0.987754E-04, A_{14}= -0.180004E-04, A_{15}=-0.358759E-05, A_{16}=+0.632672E-06, A_{17}=+0.526406E-07, A_{18}= -0.909288E-08, ε_o= 4.4566, and ε_{eu}=8.84,

$$\nu_m(\varepsilon_e)=B_1+B_2(\varepsilon_e-\varepsilon_o)+B_3(\varepsilon_e-\varepsilon_o)^2+\cdots+B_{18}(\varepsilon_e-\varepsilon_o)^{17},$$

$$\varepsilon_e \leq \varepsilon_{eu}$$

B_1=+0.307893E-01, B_2=-0.886663E-02, B_3=+0.213949E-02, B_4=-0.487063E-03, B_5=+0.952827E-04, B_6=-0.149274E-04, B_7=+0.869008E-05, B_8=-0.361783E-05, B_9=-0.808093E-06, B_{10}=+0.508998E-06, B_{11}=+0.135182E-06, B_{12}=-0.640060E-07, B_{13}=-0.859589E-08, B_{14}=+0.398899E-08, B_{15}=+0.316317E-09, B_{16}=-0.138212E-09,

B_{17}=-0.327201E-11, B_{18}=+0.172326E-11.

In the above, all A_i are in MPa, ε_o is an averaged strain, and ε_{eu} is the ultimate effective strain of the polyurethane.

5. APPLICATION

Prior to applying the bridging model to UD (unidirectional) composites, the RVE of the interlock knitted fabric reinforced composite was divided into a series of sub-cells using two parallel planes perpendicular to the wale direction[5, 6], see also Fig. 6. A sub-volume was formed from one yarn segment and the neat polyurethane matrix. Therefore, a sub-cell was imagined as two sub-volumes if two yarn segments were contained in this sub-cell. Such a sub-volume is considered as a UD fibrous composite in its local coordinate system (x_1, x_2, x_3) with x_1 along the fiber segment direction. In the present analysis, the fiber volume fractions in all such UD composites were taken to be the same, equal to the overall fiber volume fraction of the textile elastomeric composite. The micromechanical model, bridging model, described in the second section was applied to estimate the compliance matrix of the UD composite (i.e. a typical sub-volume in its local co-ordinate system). The resulting matrix was then transformed into the compliance matrix in the global co-ordinate system based on a tensor transformation rule[5,6,10] and by virtue of the yarn orientation in the RVE. The overall compliance matrix of the RVE was obtained using iso-stress condition for every sub-volume through[5,6,10]

$$[\overline{S_{ij}}] = \sum_{n=1}^{N-1} \frac{|x_{n+1}^{1st} - x_n^{1st}|}{(2L)} [\overline{S_{ij}}]_n^{1st} + \sum_{n=1}^{N-1} \frac{|x_{n+1}^{2nd} - x_n^{2nd}|}{(2L)} [\overline{S_{ij}}]_n^{2nd}$$

where (N-1) is the total number of the discretized segments of one yarn in the RVE, the superscripts 1*st* and 2*nd* stand for the first and the second yarns in the RVE, respectively, L is the projected length of one yarn on the x axis (wale direction), i.e.

$$L = |x_N^{1st} - x_1^{1st}| = |x_N^{2nd} - x_1^{2nd}|,$$

and $[\overline{S_{ij}}]_n^{1st}$ or $[\overline{S_{ij}}]_n^{2nd}$ denotes the global compliance matrix of a sub-volume.

On the other hand, if an iso-strain assumption is applied to the all sub-volumes, we have[10]

$$[\overline{C_{ij}}] = \sum_{n=1}^{N-1} \frac{|x_{n+1}^{1st} - x_n^{1st}|}{(2L)} [\overline{C_{ij}}]_n^{1st} + \sum_{n=1}^{N-1} \frac{|x_{n+1}^{2nd} - x_n^{2nd}|}{(2L)} [\overline{C_{ij}}]_n^{2nd}$$

in which $[\overline{C_{ij}}]_n^{1st}$ or $[\overline{C_{ij}}]_n^{2nd}$ denotes the global stiffness matrix of a sub-volume.

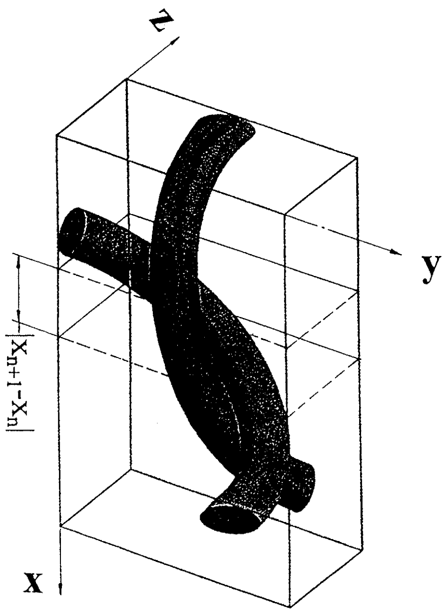

Fig. 6. A schematic diagram of subdivision for a part of RVE.

It has been shown by many authors[11,12] that iso-stress and iso-strain conditions gives two bounds for the overall properties of the composite. Hill[11] applied a combined iso-stress and iso-strain approach using a simple algebraic average. A more general approach would be a linear combination of the iso-stress assemblage with the iso-strain assemblage, from which the overall compliance matrix is simply given by

$$[\overline{S_{ij}}]^G = \alpha_c\left([\overline{C_{ij}}]^{-1}\right) + \alpha_s\left([\overline{S_{ij}}]\right), \qquad (22)$$

where α_c, $0 \le \alpha_c \le 1$, denotes the contribution ratio from the pure stiffness approach and α_s, $\alpha_s = 1 - \alpha_c$, the contribution ratio from the pure compliance approach.

Because of finite deformation, the yarn coordinates in the RVE have to be updated at the end of each load step. These coordinates are necessary for determining yarn segment orientations that are used to define the coordinate transformation matrix for the next load level calculation. In the case that the external load is unidirectionally applied along one of the global coordinate direction, the current yarn coordinates were updated according to the following formulae

$$x_i^Y = x_i^Y + (x_i^Y - x_0)d\varepsilon_x, \qquad (23)$$

$$y_i^Y = y_i^Y + (y_i^Y - y_0)d\varepsilon_y \qquad (24)$$

which only gave the averaged yarn position. In Eqs. (23) and (24), (x_0, y_0) was chosen to be the centre point of the RVE and $d\varepsilon_x$ and $d\varepsilon_y$ are the overall strain increments in wale and course directions.

It was found that taking α_c=0.9 in Eq. (22) gave the closest prediction for the linear elastic responses of the composite both in the wale and in the course directions [10]. With this same parameter, the predicted stress-strain curves in the wale and course directions are also shown in the Figs. 4 and 5. From these figures, some characteristic values are obtainable and are given in Table 1. The comparisons indicate that the agreements between the theoretical and experimental data are fairly good. This confirms that the present model is efficient.

6. CONCLUSION

A micromechanical modelling approach for predicting the mechanical properties of textile elastomeric composites is presented in this paper. The approach uses a new and accurate incremental constitutive model to describe the stress-strain behavior of the elastomer matrices. By virtue of a bridging matrix, the stress states in the constituent fiber and matrix materials are explicitly related to an overall applied load and the instantaneous compliance matrix of the composites is easily determined. The prediction can undergo as long as one of the constituent materials attains its maximum normal stress. In such case, the corresponding overall stress is taken as the ultimate strength of the composite. Two significant merits of the present approach are apparent. One is its simplicity, with no iteration and no complicated numerical calculation. Another is that internal stresses in the constituents are explicitly known, and hence the composite failure mode is clearly shown. The modeling approach has been applied to an interlock weft knitted polyester fiber fabric reinforced polyurethane elastomer matrix composite. The predicted results are in reasonably good agreement with the experimental data. Further study should focus on a more accurate description for the displaced fabric geometry when large deformation occurs.

REFERENCES

1. T. W. Chou and K. Takahashi, Composites, **18** (1987) 25.
2. K. Takahashi, T. Yano, C. M. Kuo and T. W. Chou, Trans. Japan Fiber Soc., **43** (1987) 376.
3. H. M. James and E. Guth, J. Chem. Phys., **11** (1943) 455.
4. Z. M. Huang, J. Thermoplastic Composite Materials (in press).
5. Z. M. Huang, S. Ramakrishna and A. A. O. Tay, J. of Comp. Mater. (in press).
6. Z. M. Huang, S. Ramakrishna and K. H. Leong, J. Reinf. Plastic & Comp. (in press).
7. ABAQUS---Theory Manual, Version 5.5; Example Manual, Version 5.5, Hibbitt, Karlsson & Sorensen, Inc. (1995) p. 2.2.3-1.
8. L. R. G. Treloar, Trans. Faraday Soc., **40** (1944) 59.
9. Z. M. Huang, submitted to J. Appl. Mech.
10. Z. M. Huang, S. Ramakrishna, H. P. Dinner and A. A. O. Tay, J. of Reinforced Thermoplastics & Composites, **18** (1999) 118.
11. R. Hill, Proc. Phys. Soc., **A65** (1952) 349.
12. B. Gommers, I. Verpoest and P. Van Houtte, Comp. Sci. & Tech., **56** (1996) 685.